Unique Sodium Phosphosilicate Glasses Designed Through Extended Topological Constraint Theory

ARTICLE *in* THE JOURNAL OF PHYSICAL CHEMISTRY B · APRIL 2014

Impact Factor: 3.3 · DOI: 10.1021/jp5018357 · Source: PubMed

8 AUTHORS, INCLUDING:

Huidan Zeng
East China University of Science and Technology
78 PUBLICATIONS **709** CITATIONS
SEE PROFILE

Qi Jiang
East China University of Science and Technology
9 PUBLICATIONS **27** CITATIONS
SEE PROFILE

Jing Ren
Harbin Engineering University
78 PUBLICATIONS **551** CITATIONS
SEE PROFILE

THE JOURNAL OF PHYSICAL CHEMISTRY B

Article

pubs.acs.org/JPCB

Unique Sodium Phosphosilicate Glasses Designed Through Extended Topological Constraint Theory

Huidan Zeng,*[,†] Qi Jiang,[†] Zhao Liu,[†] Xiang Li,[†] Jing Ren,[†] Guorong Chen,[†] Fude Liu,*[,‡] and Shou Peng[§]

[†]Key Laboratory for Ultrafine Materials of Ministry of Education, School of Materials Science and Engineering, East China University of Science and Technology, Shanghai 200237, China

[‡]Department of Mechanical Engineering, The University of Hong Kong, Hong Kong, China

[§]China Triumph International Engineering Company, Ltd., Shanghai 200063, China

Supporting Information

ABSTRACT: Sodium phosphosilicate glasses exhibit unique properties with mixed network formers, and have various potential applications. However, proper understanding on the network structures and property-oriented methodology based on compositional changes are lacking. In this study, we have developed an extended topological constraint theory and applied it successfully to analyze the composition dependence of glass transition temperature (T_g) and hardness of sodium phosphosilicate glasses. It was found that the hardness and T_g of glasses do not always increase with the content of SiO_2, and there exist maximum hardness and T_g at a certain content of SiO_2. In particular, a unique glass ($20Na_2O-17SiO_2-63P_2O_5$) exhibits a low glass transition temperature (589 K) but still has relatively high hardness (4.42 GPa) mainly due to the high fraction of highly coordinated network former $Si^{(6)}$. Because of its convenient forming and manufacturing, such kind of phosphosilicate glasses has a lot of valuable applications in optical fibers, optical amplifiers, biomaterials, and fuel cells. Also, such methodology can be applied to other types of phosphosilicate glasses with similar structures.

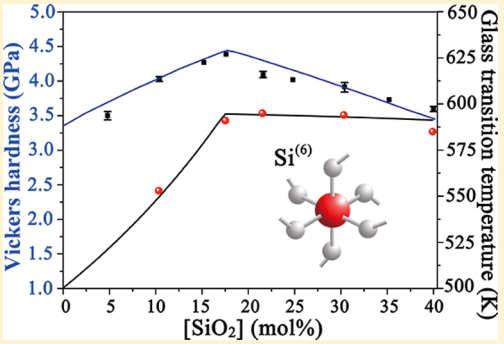

1. INTRODUCTION

Unlike phosphate or silicate glasses that have single network formers, phosphosilicate glasses have mixed network formers and then exhibit many unique properties such as excellent chemical stability, mechanical properties and photosensitivity.[1−3] Phosphosilicate glasses can be used as substrates in many applications including optical fibers,[1] optical amplifiers,[2,3] biomaterials,[3−7] and fuel cells.[8,9] A lot of efforts have been put in investigating this kind of glasses, in particular on two critical parameters: glass transition temperature (T_g) and hardness. T_g is related to the rigidity status of amorphous materials, and hardness indicates the resistance of a solid object to permanent deformation under a certain pressure. However, a proper understanding on the network structures in the glasses is lacking. In addition, a useful property-oriented methodology based on compositional changes is needed. These issues have prevented us from further improving phosphosilicate glasses in practice. Some established methods have been used for T_g simulation, including the stochastic agglomeration theory through mean coordinated number or network global connectivity[10,11] and the Vogel−Tammann−Fulcher equation through entropy.[12] While recently, temperature-dependent topological constraint theory has been developed as a powerful tool for predicting the composition dependence of physical properties at a wide range of temperatures.[13] The theoretical method focuses on the physical nature and constraints of glass structures governing thermal, mechanical and rheological properties. The success of topological constraint theory has been confirmed in both glasses with single network formers[14−16] and those with certain mixed network formers.[17,18] Therefore, the theoretical approach for predicting composition dependence of properties is expected to help the quantitative design and application of phosphosilicate glass.

In this study, theoretical simulation coupled with experimental measurements of structural and physical properties, is conducted on the nonlinear composition-dependent T_g and hardness of sodium phosphosilicate glasses. An interesting phenomenon is found that the hardness and T_g of glasses do not always increase with the content of SiO_2 as it gradually substitutes P_2O_5, but start to decrease when its content reaches a certain point. In other words, there exist maximum hardness and T_g at a certain content of SiO_2. The unexpected result is different from the traditional theory that the greater the amount of SiO_2, the greater both hardness and T_g are.

Also, the maximum value of T_g is lower compared with those in traditional glass systems, which ensures us a new glass

Received: February 21, 2014
Revised: April 21, 2014
Published: April 29, 2014

   dx.doi.org/10.1021/jp5018357 | J. Phys. Chem. B 2014, 118, 5177−5183

material that can be conveniently formed and manufactured for many applications.

2. EXPERIMENTAL SECTION

A series of $20Na_2O-xSiO_2-(80-x)P_2O_5$ (x = 4.9, 10.4, 15.3, 17.0, 21.3, 25.5, 30.4, 35.2 and 39.9, respectively) glass samples were prepared using analytical reagent-grade $NaCO_3$, $NH_4H_2PO_4$, and SiO_2 powders. For the investigation of ^{29}Si MAS NMR (=magic angle spinning nuclear magnetic resonance), additional 0.05 mol % $MnCO_3$ was added as relaxation reagent, which is not expected to affect the basic structure of glasses.[19] The mixture batches were preheated at 280 °C for 45 min before being fully melted at 1050−1250 °C for 45 min in a furnace. The melts were then casted onto a brass plate to form bulk glasses, cooled down to room temperature, and finally stored in a drying box.

The structural information on samples was obtained with MAS NMR. The MAS NMR spectra of ^{29}Si and ^{31}P were acquired with a Bruker Advance 500 MHz spectrometer. The values of T_g were determined with a differential scanning calorimetry instrument (NETZSCH STA 449F3) in nitrogen atmosphere at a heating rate of 5 K/min. The Vickers hardness (H_V) of polished glass samples was determined with micro-indentation (Wilson-Wolpert Tukon 2100B), where the indentation was performed on the sample surface at 0.98 N for 10 s.

3. RESULTS AND DISCUSSION

We first investigated the glass structure because it determines the material properties. The structural network information on typical $20Na_2O-xSiO_2-(80-x)P_2O_5$ glasses (x = 10.4, 21.2, 30.4, 39.9, respectively) can be obtained from the chemical shift of characteristic peaks shown in ^{29}Si and ^{31}P MAS NMR spectra (Figure 1a). In these glass samples, silicon atoms exist in $Si^{(4)}$ (∼−123 ppm) and $Si^{(6)}$ (∼−216 ppm) units, and phosphorus atoms in $P^{(2)}$ (∼−26 ppm) and $P^{(3)}$ (∼−37 ppm) units ($X^{(n)}$ represents the network former ion X associated with the number n of bridging oxygen atoms). Network former units (NFUs) of $Si^{(4)}$, $P^{(2)}$, and $P^{(3)}$ possess a tetrahedral structure;[19] the network former unit $Si^{(6)}$ has an octahedral structure, which is unique in sodium phosphosilicate glasses. The peaks of $Si^{(6)}$ and $P^{(3)}$ gradually become less prominent with the increase of SiO_2, and the opposite trend is true for the peaks of $Si^{(4)}$ and $P^{(2)}$; the $Si^{(4)}$ peak starts to appear when the content of SiO_2 reaches 17.0 mol % or above. Therefore, the content ratios of $Si^{(6)}/Si^{(4)}$ and $P^{(3)}/P^{(2)}$ decrease with the increase of SiO_2. The atomic fraction of each NFU is shown quantitatively in Figure 1b. Also included is the atomic fraction of sodium that is evaluated at a fixed 20 mol % of Na_2O. The fraction of $Si^{(4)}$ NFU is evaluated by multiplying the peak area percentage of $Si^{(4)}$ (=$Si^{(4)}$ peak area/($Si^{(4)}$ peak area + $Si^{(6)}$ peak area)) in the ^{29}Si MAS NMR spectra with the overall atomic fraction of Si (see Table S1 in the Supporting Information for details). The same calculation is carried out for the cases of $Si^{(6)}$, $P^{(2)}$, and $P^{(3)}$; the fraction of Na can be directly derived from the formula $20Na_2O$-$xSiO_2$-$(80-x)P_2O_5$. The evaluated values are linearly fitted to demonstrate the general trend of each structure.

The above quantitative trend may be attributed to the possible reactions in sodium phosphate glasses (Figure 2). First of all, we assume that all the sodium ions react with $P^{(3)}$ units to form $P^{(2)}$ units, which is reasonable because it is easier for sodium ions to react with $P^{(3)}$ units than $Si^{(4)}$ units—P_2O_5 has

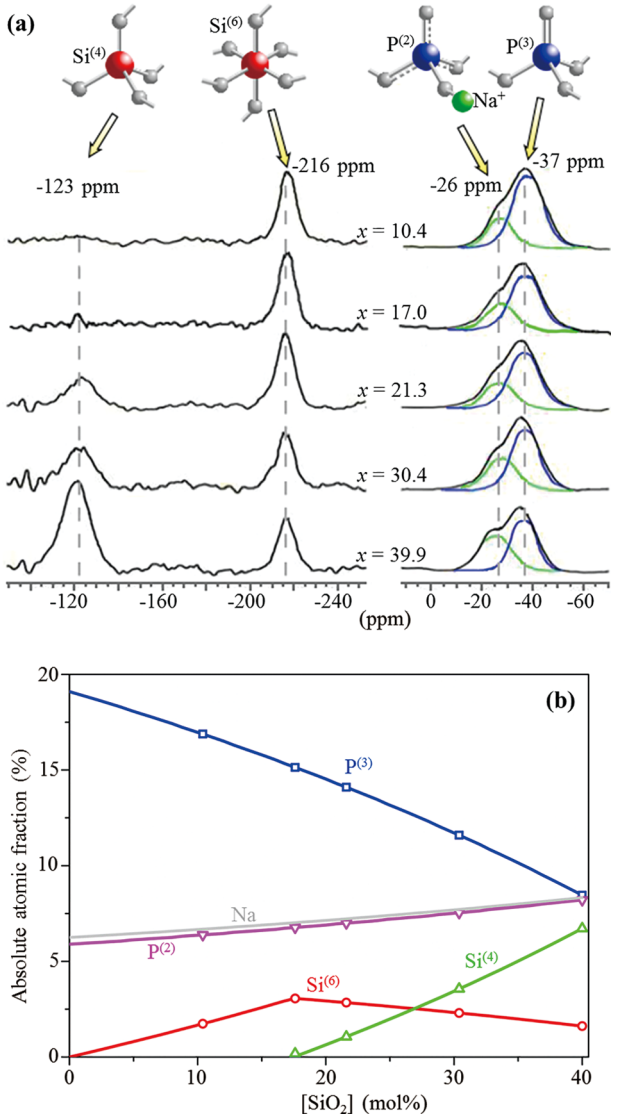

Figure 1. Structural network information on typical $20Na_2O-xSiO_2-(80-x)P_2O_5$ glasses (x = 10.4, 17.1, 21.3, 30.4 and 39.9, respectively). (a) MAS NMR spectra of $20Na_2O-xSiO_2-(80-x)P_2O_5$ glasses. The left spectra correspond to ^{29}Si and the right spectra to ^{31}P. (b) Absolute atomic fraction of each type of NFU vs SiO_2 content. The symbols represent the fraction values derived from the MAS NMR spectra and are fitted by solid lines to indicate the fraction trend. Also included is the atomic fraction of sodium that is evaluated at a fixed 20 mol % of Na_2O.

greater acid strength than SiO_2.[20] The assumption can be further validated by the experimental observation that the atomic fraction of $P^{(2)}$ almost equals that of sodium ions as shown in Figure 1b. Therefore, the atomic fraction of $P^{(3)}$ decreases as SiO_2 gradually substitutes P_2O_5, and so does the content ratio of $P^{(3)}/P^{(2)}$. On the other hand, the formation of a $Si^{(6)}$ octahedral unit is achieved when one $Si^{(4)}$ unit reacts with the nonbridging oxygen atoms of two $P^{(2)}$ units.[21] When the content of SiO_2 is less than ∼17 mol %, all $Si^{(4)}$ tetrahedrons react with sufficient $P^{(2)}$ to form $Si^{(6)}$ octahedrons. However, with more SiO_2, $P^{(2)}$ is insufficient to react with extra $Si^{(4)}$ to form $Si^{(6)}$. As a result, the ratio of $Si^{(6)}/Si^{(4)}$ decreases correspondingly with the increase of SiO_2. In addition, we should consider the effect of sodium ions during reactions. Some researchers have regarded sodium ions as charge

dx.doi.org/10.1021/jp5018357 | J. Phys. Chem. B 2014, 118, 5177−5183

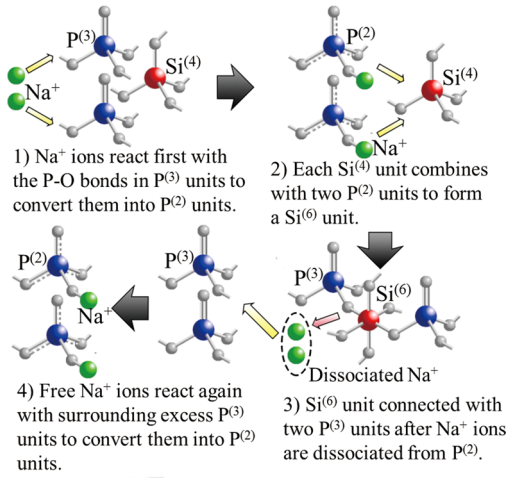

Figure 2. Possible reactions in sodium phosphate glasses.

compensators in the formation of $Si^{(6)}$ units,[22,23] which means each $Si^{(6)}$ unit should associate with two sodium ions. If this hypothesis were correct, the fraction of $P^{(2)}$ would be much less than that of sodium ions, because a significant part of sodium ions would react with $Si^{(6)}$ units instead. However, our experimental evidence shows that sodium ions completely associate with $P^{(2)}$ units as aforementioned. In fact, $Si^{(6)}$ units have been observed in $SiO_2-P_2O_5$ glass systems without network modifiers such as sodium ions.[24,25] The content fraction of $Si^{(6)}$ has been found to change and that of $P^{(2)}$ is relatively stable in sodium phosphosilicate glass series with a fixed Na_2O/P_2O_5 ratio, which indicates the close association of sodium ions with $P^{(2)}$ rather than $Si^{(6)}$.[20] After the complete formation of $Si^{(6)}$, sodium ions dissociate with $P^{(2)}$ units because the nonbridging oxygen atoms associate with $Si^{(6)}$, and then react again with surrounding excess $P^{(3)}$ units to form $P^{(2)}$ units. Overall, sodium ions enhance the formation of $Si^{(6)}$. Note that $Si^{(6)}$ should be surrounded by $P^{(2)}$ or $P^{(3)}$ rather than $Si^{(4)}$ because the covalency of Si−O−P bonds is stronger than that of Si−O−Si bonds.[22]

According to the atomic fraction trend of each NFU (see Figure 1b), the type and number of composition-dependent constraints can be obtained. Temperature-dependent topological constraint model can be used to accurately analyze T_gs of glasses. At such high temperatures as T_gs, there is sufficient thermal energy to overcome constraints to change the network to floppy modes. To calculate T_gs, the high-temperature constraints should be taken into account. There are two high-temperature constraints related to NFUs in sodium phosphosilicate glasses: α two-body constraints and β three-body constraints (their breaking temperatures follow the order of $T_\alpha > T_\beta > T_g$). The two types of constraints then remain unbroken in floppy modes. The number of constraints of each NFU obeys the rules of $\langle r/2 \rangle$ and $\langle 2r-3 \rangle$ for the two-body and three-body constraints, respectively (r represents the coordination of each NFU).[26] For α two-body constraints (Si−O and P−O), their quantity is equal to that of oxygen atoms, because each such constraint is connected to one oxygen atom only. In addition, there are two constraints associated with each oxygen atom because each oxygen atom has two single bonds. For β three-body constraints (O−Si−O and O−P−O), the number of constraints equals $(2r - 3)$. The average number of constraints for floppy modes can then be calculated by summing up the number of constraints of each NFU weighed by its atomic fraction (see Table S2 in the Supporting Information for calculated values),

$$n(x) = 2N(O, x) + 9N(Si^{(6)}, x) + 5N(Si^{(4)}, x) + 3N(P^{(3)}, x) + N(P^{(2)}, x) \quad (1)$$

The values of $N(X, x)$ for each NFU at different content of SiO_2 can be obtained from Figure 1b. The fraction of NFU, $N(X, x)$ is deduced from the ^{31}P and ^{29}Si MAS NMR experiments. The constraints due to Na atoms re not included in the present approach (eq 1). The atomic degree of freedom is related to the average number of constraints through the following relationship:

$$f(x) = d - n(x) \quad (2)$$

Here d is the maximum dimensionality for atomic free motion in network structures, i.e., the available degrees of freedom (in general, we can set $d = 3$ for glasses, a type of three-dimensional material).[13] This equation can be used for determining glass-forming ability. Because $n(x)$ is less than d, eq 2 can be used for calculating the atomic degree of freedom of glasses in floppy modes.[27] Also, the atomic degree of freedom is proportional to the configurational entropy[28,29]

$$f(x) \propto S_c(x) \quad (3)$$

where $S_c = f(x)N_A k_B \ln \Omega$, N_A is the number of atoms, k_B is the Boltzmann constant, and Ω is the number of degenerate configurations (when $f > 0$). The temperature-dependent viscosity of glasses can be determined as a function of configurational entropy through the Adam−Gibbs equation[30,31]

$$\eta = \eta_\infty \exp\left(N_A \frac{\Delta\mu}{k_B T} \frac{S_c^*}{S_c(x)}\right) \quad (4)$$

where η_∞ is the viscosity at infinite temperature and generally equals 10^{-5} Pa·s for all compositions,[32] $\Delta\mu$ is the chemical potential difference per molecule between the rearranged and nonrearranged regions, S_c^* is the molar configurational entropy of the smallest rearranged region and S_c is the molar configurational entropy of the system. $N_A(\Delta\mu/k_B)$ in the exponential term is insensitive to compositional changes for a given composition system.[33] In general, T_g is defined as the temperature at $\eta = 10^{12}$ Pa·s.[32−34] We can then get from the above eqs 2−4

$$\frac{T_g(x)}{T_g(x_R)} = \frac{S_c(x_R)}{S_c(x)} = \frac{d - n(x_R)}{d - n(x)} \quad (5)$$

where x_R represents a reference composition. Herein we set $T_g(x_R) \approx 500$ K for $20Na_2O\text{-}80P_2O_5$ glass ($x_R = 0$).[15] Since only $P^{(3)}$ and $P^{(2)}$ NFUs exist at this reference composition (see Figure 1b), we can get $n(x_R) = 2$ from eq 1 after considering only the parts of oxygen atoms, $P^{(2)}$ and $P^{(3)}$ units. With eq 5, we can get the values of T_gs for $20Na_2O-xSiO_2-(80-x)P_2O_5$ glass series (Figure 3). Overall, the calculated T_gs are in good agreement with experimental ones. We see that T_g increases rapidly when SiO_2 increases from 0 mol % to 17 mol %, and then declines slowly afterward.

Topological constraint theory can also be used for predicting the hardness of glass samples. Glass hardness is closely related to the structures of internal network formers. In terms of chemical bond characteristics of network formers, P−O and Si−O have quite similar bond strength and length.[21] Because it

dx.doi.org/10.1021/jp5018357 | J. Phys. Chem. B 2014, 118, 5177−5183

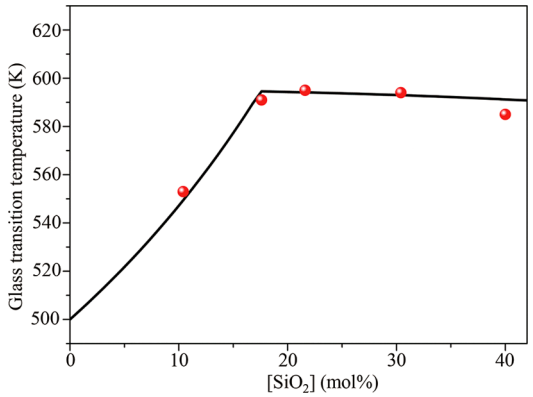

Figure 3. Glass transition temperature vs SiO_2 content for $20Na_2O-xSiO_2-(80-x)P_2O_5$ glasses. The solid line and sphere symbols represent the model-predicted results and experimental data, respectively.

is challenging to tell the exact contribution of chemical bonds to macroscopic hardness, the constraints associated with glass structures can be used to solve this issue. According to the topological constraint theory, we have the following equation:[35]

$$H_V(x) = \left(\frac{dH_V}{dn'}\right)[n'(x) - n_{crit}] \quad (6)$$

Because the hardness is measured at room temperature that is much lower than T_g (glasses are stressed-rigid now), we need to consider other low-temperature constraints as well. Thus, to calculate the average number of constraints $n'(x)$ at room temperature, we should consider other γ three-body constraints (P−O−P and S−O−P) that are unbroken at room temperature (the breaking temperatures follow the order of $T_{room} < T_\gamma < T_g < T_\beta < T_\alpha$). For these γ three-body constraints, each oxygen atom is associated with one more constraint. eq 1 can then be modified to be

$$n'(x) = 3N(O, x) + 9N(Si^{(6)}, x) + 5N(Si^{(4)}, x) + 3N(P^{(3)}, x) + N(P^{(2)}, x) \quad (7)$$

The calculated values of $n'(x)$ (Table S2) are less than 3 but greater than the critical count, n_{crit} (Table S2, and Discussion below) used as a measure to establish hardness of glasses at room temperature.[27] With experimental values of hardness, we can then plot the hardness as a function of $n'(x)$ at room temperature (Figure 4a). With eq 6, we can further fit the data with a straight line. The value of (dHv/dn') is derived to be ~11.3 GPa.

The critical number of constraints (n_{crit}) is another important parameter that is determined by the dimension of material networks. n_{crit} = 2 for a chain network that is rigid along one dimension, n_{crit} = 2.5 for a layer structural material such as graphite due to the weak interactions between layers, and n_{crit} = 3 for a network being full rigid in three dimension.[35] For glass materials, the values of n_{crit} have been reported only for borate and borosilicate glasses.[17,35] For single-network-former glasses containing limited types of NFUs, the predicted values of hardness with n_{crit} = 2.5 have been shown to be in good agreement with experimental values.[35] For glasses with mixed network formers, great discrepancy (>10%) exists for the predicted hardness if n_{crit} = 2.5.[17] Because of the composition changes, mixed-network-former glasses may have various dimensional degrees of rigid networks. So the n_{crit} value of each NFU should be analyzed individually. n_{crit} = 2 for a $P^{(2)}$ chain structure. For a $P^{(3)}$ unit, we can set n_{crit} = 2.5, because there are a P═O double bond and three bridging oxygen atoms located on the same plane. Because there is no nonbridging oxygen atom associated with $Si^{(4)}$ and $Si^{(6)}$ units, we have n_{crit} = 3 for both type of units. Consequently, the values of n_{crit} for our $20Na_2O$-$xSiO_2$-$(80-x)P_2O_5$ glasses can be obtained with the following equation,

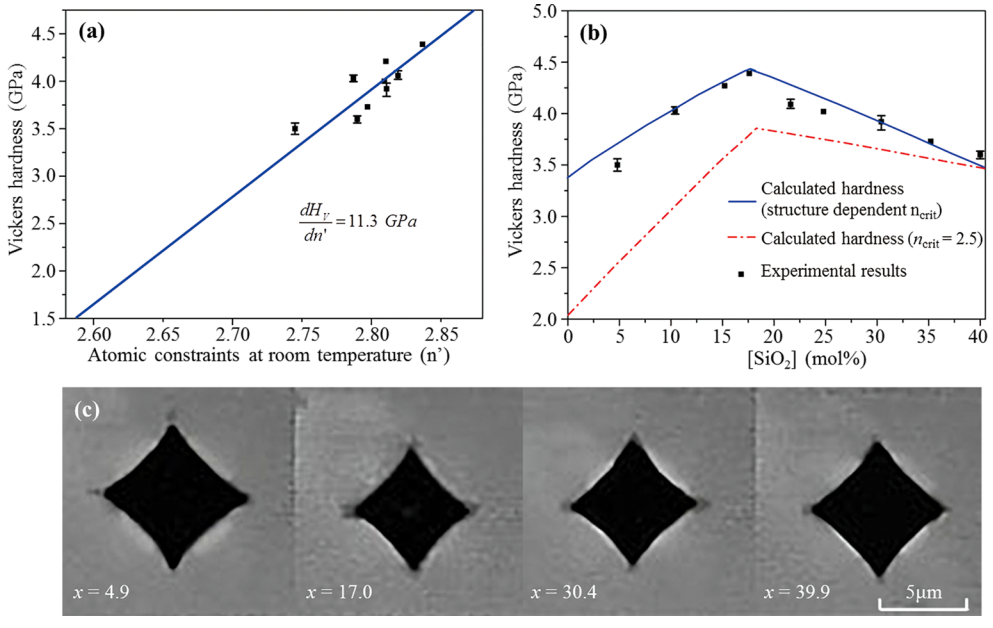

Figure 4. Hardness of $20Na_2O-xSiO_2-(80-x)P_2O_5$ glass series. (a) Vickers hardness as a function of the number of atomic constraints at room temperature. Also shown is the calculated slope value of 11.3 GPa. (b) Experimental and calculated (with eq 6) Vickers hardness as a function of SiO_2 content. The solid line and dash line correspond to the calculated hardness of the case of structure-dependent n_{crit} and the case of fixed n_{crit} (=2.5), respectively. (c) Images of indentations measured at a load of 0.98 N when x = 4.9, 17.0, 30.4 and 39.9, respectively.

dx.doi.org/10.1021/jp5018357 | J. Phys. Chem. B 2014, 118, 5177−5183

$$n_{crit} = 3N'(Si^{(6)}, x) + 3N'(Si^{(4)}, x) + 2.5N'(P^{(3)}, x) + 2N'(P^{(2)}, x) \quad (8)$$

where N' represents the percentage of each NFU among all the NFUs, for example, $N'(Si^{(6)},x)$ = fraction of $Si^{(6)}$/ fraction of ($Si^{(6)}$+ $Si^{(4)}$+ $P^{(3)}$+ $P^{(2)}$) (fraction values can be obtained directly from Figure 1b). The calculated values of n_{crit} for $20Na_2O-xSiO_2-(80-x)P_2O_5$ glasses are shown in Table S2 in the Supporting Information. The Vickers hardness of sodium phosphosilicate glass series can then be calculated as a function of SiO_2 content with eq 6 (Figure 4b). The solid line and dash line correspond to the case of structure dependent n_{crit} and the case of fixed n_{crit} (=2.5), respectively. Compared with the latter, the former fits experimental values much better. The hardness increases with the content of SiO_2 until it reaches the maximum at ~17 mol % SiO_2, and then decreases with more SiO_2. This observation can be further confirmed with the images of indentations (Figure 4c). The indentation becomes smaller with the increase of SiO_2 content, and then it starts to enlarge with more SiO_2.

We see that both T_g and hardness of sodium phosphosilicate glasses are closely related to the average number of constraints. $Si^{(6)}$ octahedral units are related to β constraints that are nine times as many as the former units, and are far more than the constraints associated with other types of NFUs. Therefore, the increase of highly coordinated $Si^{(6)}$ units contributes greatly to the rapid increase of T_gs and hardness when the SiO_2 content is <~17 mol %. However, with further increase of SiO_2, both T_g and hardness decrease (at different paces though) because $Si^{(4)}$ starts to substitute $Si^{(6)}$. Obviously the fraction of $Si^{(6)}$ units can greatly affect the T_g and hardness of sodium phosphosilicate glasses.

Finally we compare our sodium phosphosilicate glass containing 17 mol % SiO_2 (i.e., $20Na_2O-17SiO_2-63P_2O_5$) with traditional glass systems (Figure 5).[36−45] In general, glasses with high T_g also possess strong hardness and vice versa (see the color band area shown in Figure 5). However, as highlighted by a red star in the figure, our glass of $20Na_2O$-$17SiO_2$-$63P_2O_5$ is unique because it has a low T_g (589 K)[41] but still has high hardness (4.42 GPa) mainly due to the high fraction of $Si^{(6)}$. Therefore, by applying the extended topological constraint theory, we can really achieve a glass system with strong hardness but still low T_g. In principle, such methodology can be applied to other types of phosphosilicate glasses with similar structures,[46−48] and mechanical properties.[49]

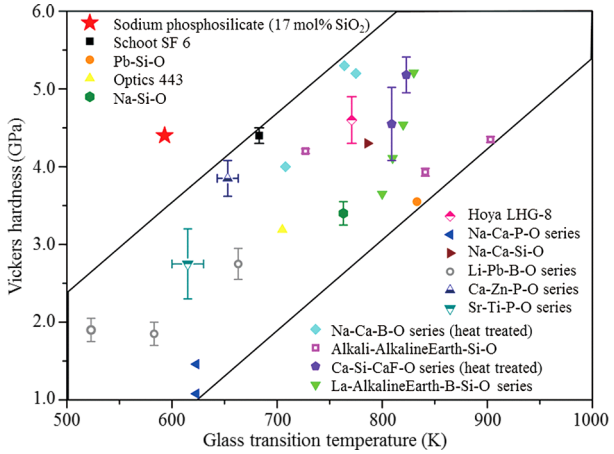

Figure 5. Relationship between hardness and glass transition temperature (T_g) in typical glasses.[36−45]

4. CONCLUSIONS

In summary, topological constraint theory has been successfully applied to analyze the composition dependence of T_g of sodium phosphosilicate glasses; with some modifications, the theory has been extended to study the hardness as well. The calculated values of T_g and hardness are in good agreement with experimental ones. It was found that the hardness and T_g of glasses do not always increase with the content of SiO_2 and there exist maximum hardness and T_g at a certain content of SiO_2, which was found to be mainly related to the constraints originated from 6-fold coordinated silicon NFUs ($Si^{(6)}$). In particular, the sodium phosphosilicate glass with 17 mol % SiO_2 exhibits a low T_g (589 K) but still has relatively high hardness (4.42 GPa). Because of its convenient forming and manufacturing, such kind of phosphosilicate glasses has a lot of potential applications in many fields including optical fibers, optical amplifiers, biomaterials, and fuel cells. Also, such methodology can be applied to other types of phosphosilicate glasses with similar structures.

■ ASSOCIATED CONTENT

Supporting Information

Additional information on the MAS NMR and modeling. This material is available free of charge via the Internet at http://pubs.acs.org.

■ AUTHOR INFORMATION

Corresponding Authors

*(H.Z.) E-mail: hdzeng@ecust.edu.cn. Telephone: (+86) 21-64253395. Fax: (+86) 21-64253395.

*(F.L.) E-mail: fordliu@hku.hk. Telephone: (+852) 2859 2631. Fax: (+852) 2858-5415.

Notes

The authors declare no competing financial interest.

■ ACKNOWLEDGMENTS

This work was supported by the Natural Science Foundation of Shanghai (12ZR1407600), the Fundamental Research Funds for the Central Universities, the Shanghai Leading Academic Discipline Project (B502). We would like to thank Dr. Jiacheng Li (The Shanghai Institute of Ceramics, Chinese Academy of Sciences) and Guangjun Zhang (Schott Glass Technology (Suzhou) Co., Ltd) for stimulating discussion about glass structure.

■ REFERENCES

(1) Canning, J.; Sommer, K.; Englund, M.; Huntington, S. Direct Evidence of Two Types of UV-Induced Glass Changes in Silicate-Based Optical Fibers. *Adv. Mater.* **2001**, *13*, 970−973.

(2) Fujii, M.; Mimura, A.; Hayashi, S.; Yamamoto, K. Photoluminescence from Si Nanocrystals Dispersed in Phosphosilicate Glass Thin Films: Improvement of Photoluminescence Efficiency. *Appl. Phys. Lett.* **1999**, *75*, 184−186.

(3) Aronne, A.; Torco, M.; Bagnasco, G.; Pernice, P.; Serio, M. D.; Clayden, N. J.; Marenna, E.; Fanelli, E. Synthesis of High Surface Area Phosphosilicate Glasses by A Modified Sol-Gel Method. *Chem. Mater.* **2005**, *17*, 2081−2090.

(4) Duée, C.; Grattepanche-Lebecq, I.; Désanglois, F.; Follet-Houttemane, C.; Chai, F.; Hildebrand, H. F. Predicting Bioactive Properties of Phosphosilicate Glasses Using Mixture Designs. *J. Non-Cryst. Solids* **2013**, *362*, 47−55.
(5) Lusvardi, G.; Zaffe, D.; Menabue, L.; Bertoldi, C.; Malavas, G.; Consolo, U. In Vitro and In Vivo Behaviour of Zinc-Doped Phosphosilicate Glasses. *Acta Biomater.* **2009**, *5*, 419−428.
(6) Barth, B. M.; Sharma, R.; Altınoglu, E. I.; Morgan, T. T.; Shanmugavelandy, S. S.; Kaiser, J. M.; McGovern, C.; Matters, G. L.; Smith, J. P.; Kester, M.; et al. Bioconjugation of Calcium Phosphosilicate Composite Nanoparticles for Selective Targeting of Human Breast and Pancreatic Vancers In Vivo. *ACS Nano* **2010**, *4*, 1279−1287.
(7) Morgan, T. T.; Goffb, T. M.; Adair, J. H. The Colloidal Stability of Fluorescent Calcium Phosphosilicate Nanoparticles: The Effects of Evaporation and Redispersion on Particle Size Distribution. *Nanoscale* **2011**, *3*, 2044−2053.
(8) Lim, J.; Won, J.; Lee, H.; Hong, Y. T.; Lee, M.; Koand, C. H.; Lee, S. Polyimide Nonwoven Fabric-Reinforced, Flexible Phosphosilicate Glass Composite Membranes for High-Temperature/Low-Humidity Proton Exchange Membrane Fuel Cells. *J. Mater. Chem.* **2012**, *22*, 18550−18557.
(9) Li, H.; Chen, X.; Jiang, F.; Ai, M.; Di, Z.; Gu, J. Flexible Proton-Conducting Glass-Based Composite Membranes for Fuel Cell Application. *J. Power Sources* **2012**, *199*, 61−67.
(10) Micoulaut, M. The Slope Equations: A Universal Relationship between Local Structure and Glass Transition Temperature. *Eur. Phys. J. B* **1998**, *1*, 277−294.
(11) Micoulaut, M.; Naumis, G. G. Glass Transition Temperature Variation, Cross-Linking and Structure in Network Glasses: A Stochastic Approach. *Europhys. Lett.* **1999**, *47*, 568−574.
(12) Angell, C. A.; Smith, D. L. Test of the Entropy Basis of the Vogel-Tammann-Fulcher Equation. Dielectric Relaxation of Polyalcohols near Tg. *J. Phys. Chem.* **1982**, *86*, 3845−3852.
(13) Gupta, P. K.; Mauro, J. C. Composition Dependence of Glass Transition Temperature and Fragility. I. A Topological Model Incorporating Temperature-Dependent Constraints. *J. Chem. Phys.* **2009**, *130*, 094503.
(14) Mauro, J. C.; Gupta, P. K.; Loucks, R. J. Composition Dependence of Glass Transition Temperature and Fragility. II. A Topological Model of Alkali Borate Liquids. *J. Chem. Phys.* **2009**, *130*, 234503.
(15) Fu, A. I.; Mauro, J. C. Topology of Alkali Phosphate Glass Networks. *J. Non-Cryst. Solids* **2013**, *361*, 57−62.
(16) Smedskjaer, M. M.; Mauro, J. C.; Sen, S.; Yue, Y. Quantitative Design of Glassy Materials Using Temperature-Dependent Constraint Theory. *Chem. Mater.* **2010**, *22*, 5358−5365.
(17) Smedskjaer, M. M.; Mauro, J. C.; Youngman, R. E.; Hogue, C. L.; Potuzak, M.; Yue, Y. Topological Model for the Viscosity of Multicomponent Glass-Forming Liquids. *J. Phys. Chem. B* **2011**, *115*, 12930−12946.
(18) Jiang, Q.; Zeng, H.; Liu, Z.; Ren, J.; Chen, G.; Wang, Z.; Sun, L.; Zhao, D. Glass Transition Temperature and Topological Constraints of Sodium Borophosphate Glass-Forming Liquids. *J. Chem. Phys.* **2013**, *139*, 124502.
(19) Dupree, R.; Holland, D.; Mortuza, M. G. Six-Coordinated Silicon in Glasses. *Nature* **1987**, *328*, 416−417.
(20) Yamashita, H.; Yoshino, H.; Nagata, K.; Yamaguchi, I.; Ookawa, M.; Maekawa, T. NMR and Raman Studies of Na_2O-P_2O_5-SiO_2 Glasses. *J. Ceram. Soc. Jpn.* **1998**, *106*, 539−544.
(21) Miyabe, D.; Takahashi, M.; Tokuda, Y.; Yoko, T.; Uchino, T. Structure and Formation Mechanism of Six-Fold Coordinated Silicon in Phosphosilicate Glasses. *Phys. Rev. B* **2005**, *71*, 172202.
(22) Li, D.; Fleet, M. E.; Bancroft, G. M.; Kasrai, M.; Pan, Y. Local Structure of Si and P in SiO_2-P_2O_5 and Na_2O-SiO_2-P_2O_5 Glasses: A XANES Study. *J. Non-Cryst. Solids* **1995**, *188*, 181−189.
(23) Dupree, R.; Holland, D.; Mortuza, M. G.; Collins, J. A.; Lockyer, M. W. G. An MAS NMR Study of Network-Cation Coordination in Phosphosilicate Glasses. *J. Non-Cryst. Solids* **1988**, *106*, 403−407.
(24) Weeding, T. L.; de Jong, B. H. W. S.; Veeman, W. S.; Aitken, B. G. Silicon Coordination Changes from 4-Fold to 6-Fold on Devitrification of Silicon Phosphate Glass. *Nature* **1985**, *318*, 352−353.
(25) Sakida, S.; Nanba, T.; Miura, Y. Structural Change around Si Atoms in P_2O_5-SiO_2 Binary Glasses before and after Annealing by ^{29}Si MAS NMR Spectroscopy. *Chem. Lett.* **2006**, *35*, 1268−1269.
(26) Phillips, J. C. Topology of Covalent Non-Crystalline Solids. I. Short-Range Order in Chalcogenide Alloys. *J. Non-Cryst. Solids* **1979**, *34*, 153−181.
(27) Phillips, J. C.; Thorpe, M. F. Constraint Theory, Vector Percolation and Glass Formation. *Solid State Commun.* **1985**, *53*, 699−702.
(28) Naumis, G. G. Energy Landscape and Rigidity. *Phys. Rev. E* **2005**, *71*, 026114.
(29) Naumis, G. G. Variation of the Glass Transition Temperature with Rigidity and Chemical Composition. *Phys. Rev. B* **2006**, *73*, 172202.
(30) Adam, G.; Gibbs, J. H. On the Temperature Dependence of Cooperative Relaxation Properties in Glass-Forming Liquids. *J. Chem. Phys.* **1965**, *43*, 139−146.
(31) Toplis, M. J. Energy Barriers to Viscous Flow and the Prediction of Glass Transition Temperatures of Molten Silicates. *Am. Mineral.* **1998**, *83*, 480−490.
(32) Angell, C. A. Spectroscopy Simulation and Scattering, and the Medium Range Order Problem in Glass. *J. Non-Cryst. Solids* **1985**, *73*, 1−17.
(33) Angell, C. A. Structural Instability and Relaxation in Liquid and Glassy Phases Near the Fragile Liquid Limit. *J. Non-Cryst. Solids* **1988**, *102*, 205−221.
(34) Angell, C. A. Relaxation in Liquids, Polymers and Plastic Crystals — Strong/Fragile Patterns and Problems. *J. Non-Cryst. Solids* **1991**, *131*−*133*, 13−31.
(35) Smedskjaer, M. M.; Mauro, J. C.; Yue, Y. Prediction of Glass Hardness Using Temperature-Dependent Constraint Theory. *Phys. Rev. Lett.* **2010**, *105*, 115503.
(36) Sellappan, P.; Rouxel, T.; Celarie, F.; Becker, E.; Houizot, P.; Conradt, R. Composition Dependence of Indentation Deformation and Indentation Cracking in Glass. *Acta Mater.* **2013**, *61*, 5949−5965.
(37) Pollington, S.; van Noort, R. Manufacture, Characterisation and Properties of Novel Fluorcanasite Glass−Ceramics. *J. Dent.* **2012**, *40*, 1006−1017.
(38) Sinouh, H.; Bih, L.; Azrour, M.; ElBouari, A.; Benmokhtar, S.; Manoun, B.; Belhorma, B.; Baudin, T.; Berthet, P.; Haumont, R.; et al. Elaboration and Structural Characterization of Glasses Inside the Ternary SrO-TiO_2-P_2O_5 System. *J. Phys. Chem. Solids* **2012**, *73*, 961−968.
(39) Kashif, I.; El-Maboud, A. A.; El-said, R.; Sakr, E. M.; Soliman, A. A. The Role of Lead Oxide on Structural and Physical Properties of Lithium Diborate Glasses. *J. Alloys Compd.* **2012**, *539*, 124−128.
(40) Ghosh, S.; Ghosh, A.; Kar, T.; Das, S.; Das, P. K.; Banerjee, R. Cushioning Effect, Enhanced Localized Plastic Flow and Thermal Transport in SWCNT−Lead Silicate Glass Composite. *Chem. Phys. Lett.* **2012**, *547*, 58−62.
(41) Marino, A. E.; Arrasmith, S. R.; Gregg, L. L.; Jacobs, S. D.; Chen, G. R.; Duc, Y. J. Durable Phosphate Glasses with Lower Transition Temperatures. *J. Non-Cryst. Solids* **2001**, *289*, 37−41.
(42) Marikani, A.; Maheswaran, A.; Premanathan, M.; Amalraj, L. Synthesis and Characterization of Calcium Phosphate Based Bioactive Quaternary P_2O_5−CaO−Na_2O−K_2O Glasses. *J. Non-Cryst. Solids* **2008**, *354*, 3929−3934.
(43) Kaur, G.; Pandey, O. P.; Singh, K. Effect of Modifiers Field Strength on Optical, Structural and Mechanical Properties of Lanthanum Borosilicate Glasses. *J. Non-Cryst. Solids* **2012**, *358*, 2589−2596.
(44) Hermansen, C.; Matsuoka, J.; Yoshida, S.; Yamazaki, H.; Kato, Y.; Yue, Y. Z. Densification and Plastic Deformation under Microindentation in Silicate Glasses and the Relation to Hardness and Crack Resistance. *J. Non-Cryst. Solids* **2013**, *364*, 40−43.

(45) Striepe, S.; Smedskjaer, M. M.; Deubener, J.; Bauer, U.; Behrens, H.; Potuzak, M.; Youngman, R. E.; Mauro, J. C.; Yue, Y. Z. Elastic and Micromechanical Properties of Isostatically Compressed Soda−Lime−Borate Glasses. *J. Non-Cryst. Solids* **2013**, *364*, 44−52.
(46) Stebbins, J. F.; Kanzaki, M. Local Structure and Chemical Shifts for Six-Coordinated Silicon in High-Pressure Mantle Phases. *Science* **1991**, *251*, 294−298.
(47) Tofield, B. C.; Crane, G. R.; Bridenbaugh, P. M.; Sherwood, R. C. Novel Phosphosilicate. *Nature* **1975**, *253*, 722−723.
(48) Dent, L. S.; Smith, D. N. On the Occurrence of Phosphosilicates. *Nature* **1978**, *274*, 878−879.
(49) Wondraczek, L.; Mauro, J. C.; Eckert, J.; Kühn, U.; Horbach, J.; Deubener, J.; Rouxel, T. Towards Ultrastrong Glasses. *Adv. Mater.* **2011**, *23*, 4578−4586.